INVESTIGATION OF ATTENUATION AND BLOCKAGE OF LG IN THE VICINITY OF THE KYRGYZ ARRAY

Vernon F. Cormier and Tom Anderson
Department of Geology and Geophysics
University of Connecticut
Storrs, CT 06269-2045

F49620-94-1-0059
Sponsored by AFOSR

ABSTRACT:

Synthetic seismograms and ray paths obtained by 3-D dynamic ray tracing are compared with regional seismograms from the KNET array in the Republic of Kyrgyzstan, in the former Soviet Union. Variations in regional waveforms recorded by the KNET array in the Republic of Kyrgyzstan are compared with predicted variations in the paths of multiple SmS waves comprising the Lg phase using the database of Moho topography by Fielding et al. (1993). Ray diagrams predict strong regional variations Lg efficiency in Kyrgyz area. The strongest variations in observed Lg amplitudes and predicted Lg paths are associated with strong gradients in Moho topography along the Hindu Kush and Pamir mountain ranges. Lg is nearly extinguished for paths from shallow events to the southwest of the Kyrgyz array, which traverse regions of strong Moho gradient. Detailed variations of waveforms across the Kyrgyz array are consistent with Lg efficiency being proportional to the length and number of times SmS ray paths traverse regions of strong Moho gradient. Synthetic seismograms predict that crustal thickness variations will either compress or stretch the Lg coda compared to that predicted in a crust of uniform thickness.

OBJECTIVE:

The crust and uppermost mantle are the most strongly laterally varying and heterogeneous regions of the Earth. The seismic phases Pn, Pg, Sn, Lg, and Rg, which are important to nuclear verification of small sources, are all strongly affected by this heterogeneity, complicating the transportability of methods to detect, discriminate and yield estimate in different regions. There is a need to predict the effects of heterogeneous crustal structure on regional phase propagation using geological and geophysical information for regions in which little or no seismic recording has occurred. The computational expense of a numerical solution of the wave equation in an arbitrarily heterogeneous model have thus far limited such predictions to primarily 2-D structure and low frequency bands. Ray based techniques of forward modeling, however, are sufficiently fast to allow practical predictions of efficiency of the propagation of regional phases in detailed 3-D structures. The effects of scattering by statistically distributed heterogeneity can also be incorporated in ray methods by single scattering theory. The objective of this project is to develop and apply the methods of dynamic ray tracing and superposition of Gaussian beams to forward model regional seismic phases in three-dimensionally varying models of the Earth's crust. Goals include (a) an understanding of what crustal structures are most important in determining the efficiency of regional phase propagation, (b) determining what type of non-seismic data (topography, surficially mapped geology, gravity, magnetics) are most useful in inferring 3-D crustal structure, and (c) testing the success of a fast ray-based modeling procedure in modeling detailed features of regional waveform

RESEARCH ACCOMPLISHED:

Crustal Models and Dynamic Ray Tracing

Regional seismograms are synthesized by summing dynamically traced rays and/or superposing Gaussian beams (e.g., Cerveny, 1985) in models of the crust for the vicinity of the Kyrgyz array. Moho turning points of the rays comprising the Lg and Pg phase are projected in a map view to illustrate predicted efficiency of propagation. To simplify the description of rays and reduce model storage, the model parameters are assumed to be continuous functions of space. P and S velocity and density are parameterized by functions:

$$v(x,y,z) = a + b\tanh(z - h_1(x,y)/s_1) + c\tanh(z - h_2(x,y)/s_2)$$

where $h_1(x,y)$ and $h_2(x,y)$ specify the depth of the sedimentary basin/basement contact and depth of the Moho, respectively. The functions h_1 and h_2 are given as continuous functions of horizontal coordinates by interpolating digitized surfaces by splines under tension. Additional tanh functions can be added, as needed, to model more interfaces. In the vicinity of the Kyrgyz array, h_1 and h_2 are taken from databases assembled by Fielding et al. (1993). A plot of ray trajectories useful in the interpretation of structural effects on Lg. A useful plot is a map view of SmS turning points and surface bounce points (Bostock and Kennett, 1991). Several of these types of plots are discussed in the interpretation of Kyrgyz data.

Data Interpretation

Regional data shown were recorded in Kyrgyzstan by a 10 station network that was installed in the summer of 1991 (JSPC, 1993). Stations EKS2 and TKM are located on piers in underground vaults. Station AAK is located approximately 40 m inside a tunnel constructed specifically for geophysical observations. Station CHM s located in a small building at the bottom of a hill.

Events were selected based on the following criteria: shallow depth and published JSPC location. (JSPC locations are more precise than the PDE locations for the events in this region.) Events are selected in the distance range 300 to 1200 km. in epicentral distance. From the events that met these criteria, four were chosen based on the quality and azimuthal paths that traversed regions of strong Moho topography in the Fielding database (figures 1b-c).

Data are band pass filtered from .5 to 5 Hz. using a butterworth filter with 4 poles. The data are displayed in record section plots in SAC.

Event 3. 25 Mar 92. This event traverses a region of Moho east of the array that is relatively flat and 47 km deep (figures1a-c). The record sections (figure 2) show similarities in both Lg coda length, shape, and amplitude ratio to Pg. The similarities in Lg coda are consistent with the expected effect of the flat Moho between the source and array. Dynamic ray tracing shows that the rays passing through this region are not greatly affected by the slight changes in Moho topography. The ray tracing results (figures 3 ,4) are shown in map view of SmS bounce points and 2-D cross sections of ray paths projected onto vertical planes through the back azimuths to stations. Figure 3 shows relatively coherent wavefronts of bounce points reaching out to the Kyrgyz array. The rays calculated for this event shown in figure 4 illustrate that in a region of nearly flat Moho, the rays remain coherent over regional distances, in this case out to approximately 600 km. At longer range, figure 4 and subsequent ray plots show that many rays experience azimuthal bending.

Event 1. 6 May 92. This event was chosen for the ray paths that pass through a region north of the Pamir Mountains where the depth of the Moho increases to 70 km with steep gradients. The array had a back azimuthal range (baz) of 198.02-209.86 degrees and ranged in distance from 527.91-611.25 km. The effects of the steep Moho gradients are seen in the Lg which differs greatly across the array (figure 5). Station TKM (baz 209.86 dist 599 km) shows almost no sign of Lg coda, station CHM (baz 204.86 dist. 592 km) has very little Lg, while AAK(baz 204.47 dist 546km) has noticeable Lg and station EKS2 (baz 198.02; dist. 527km) has significant Lg. Ray tracing shows similarly strong variations for rays passing this region. The map view (figure 6) of ray bounce points for this source receiver scenario shows that the wave front is distorted by the second bounce and a 2-D caustic develops which transects the array. This correlates well with the differences seen in Lg from one side of the array to the other. Two-dimensional vertical cross sections of rays for this event (figure 7) illustrate the same degree of variation. The rays diverge after the first bounce and the ‘range of coherency’ can be said to be less than 100 km.

Event 2. 27 Jun 92. The array had a back azimuthal range of 139.17-146.57 degrees and ranged in distance from 987-1047 km. This event originated over the deep Moho b(70 km) associated with the Hindu Kush region. The record section plot (figure 8) shows the variation across the array in Lg coda shape and amplitude ratio to Pg consistent with the changes in Moho topography. The Lg coda at station EKS2 has a different shape and a much lower Lg/Pg ratio than the rest of the array. The ray tracing depicts similar effects from the Moho gradients in this region. The map view of SmS bounce points (figure9) shows the distortion of the wavefront as it crosses the Moho and a 2-d caustic aligned over station EKS2. The ray tracing (figure 10) shows rays shot at azimuths to the stations EKS2 and TKM. The slight difference in azimuth yields totally different ray paths through this region.

RECOMMENDATIONS AND FUTURE PLANS:

Ray synthetics in simple crustal models do not have the complexity exhibited in recorded Lg coda. Realistic complexity can be introduced by fine plane layering in 1-D structure. It would be a mistake, however, to attribute the observed complexity to 1-D structure even if good matches between observed and synthetic waveforms can be obtained. Array analysis of regional phases have made it clear that the coda of regional phases contains scattered arrivals, including energy arriving off-azimuth.

Up to frequencies as high as 5 Hz, the details of local S coda can be well explained by first order scattering by heterogeneities distributed within the crust and uppermost mantle. In the poster accompaning this paper, the results of experiments in modeling the realistic complexity of Lg coda are shown using a first-order Born approximation. Experiments are shown using single scattering incorporated in a superposition of locked modes. Future experiments will include single scattering in the ray approached described in this paper. A recommended approach to modeling the effects of 3-D structure on regional seismograms would be a ray approach to include the effects of large scale deterministic structures, such as Moho topography having scale lengths greater than 10 km, coupled with single scattering theory applied to small scale statistical structure.

CONCLUSIONS AND RECOMMENDATIONS:

Synthetics and ray diagrams predict the strong regional variations in Lg efficiency seen in data collected at the Kyrgyz array. The plots of SmS turning points for the events in this study strongly suggests that a strong transition Lg amplitudes occurs for paths traversing regions of strong Moho gradient along the Hindu Kush and Pamir mountains. A common effect of crustal thickness variation is either compression or stretching of the Lg coda compared to that predicted in a crust of uniform thickness. It may be possible to incorporate this effect in the refinement of regional discriminants.

REFERENCES:

Bostock, M.G., and B.L.N. Kennett, The effect of 3-dimensional structure on Lg propagation patterns, *Geophys. J. Int.*, 355-365, 1991.

Cerveny, V., The application of ray tracing to the propagation of shear waves in complex media, in *Seismic Exploration* pp. 1-124, Treitel and Helbig, Vol. on Seismic Shear Waves, G. Dohr, ed., Geophysical Press, 1985.

Fielding, E., M. Barazangi, and B. Isacks, A network-accessible geological and geophysical database for Eurasia, North Africa, and the Middle East, *Proceedings 15th Annual Seismic Research Symposium*, AFOSR/DARPA, PL-TR-93-2160, ADA-271458, 1993

Joint Seismic Program Center, Kyrgyz Network Information Product, Technical Reference Manual, Version 1.0, 1993.

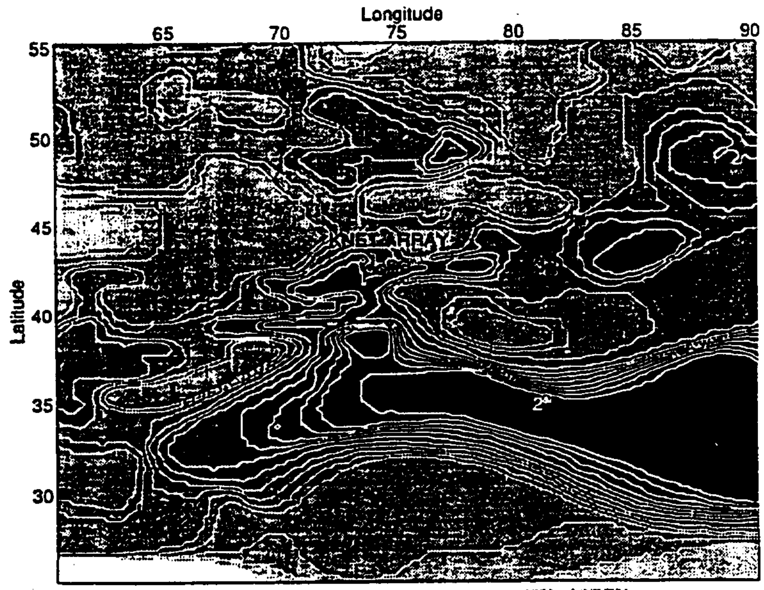

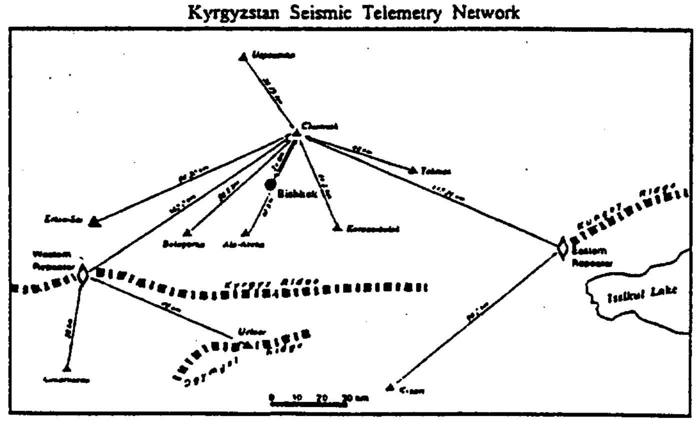

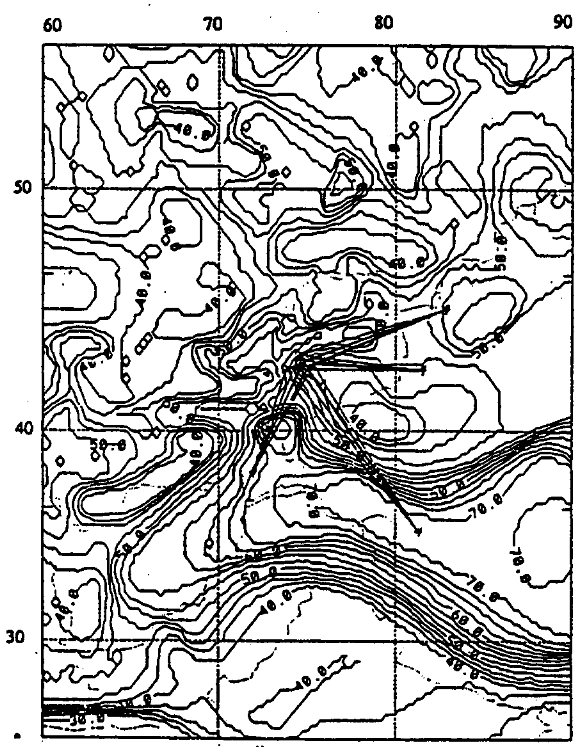

Figure 1. (a) Top left: Kyrgyz array and events on a contour map of Moho topography. (b) Top right: Kyrgyz seismic network (JSPC KNET technical reference manual). (c) Bottom: contour map of Moho topography with 4 events in this study.

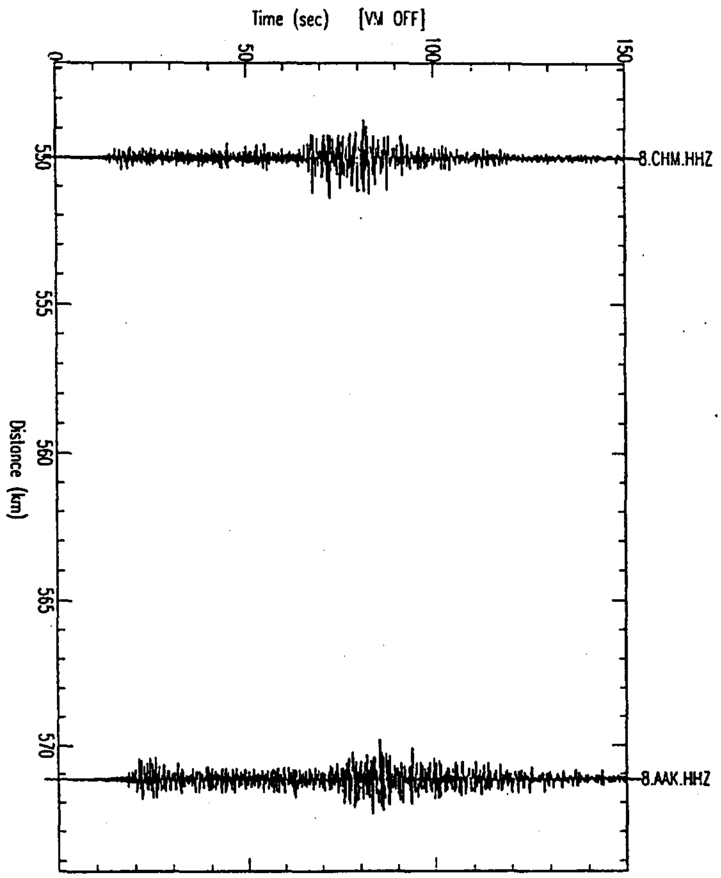

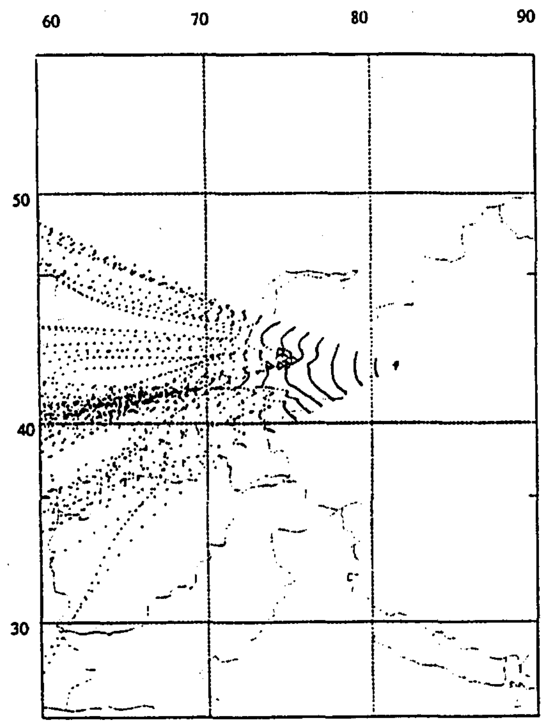

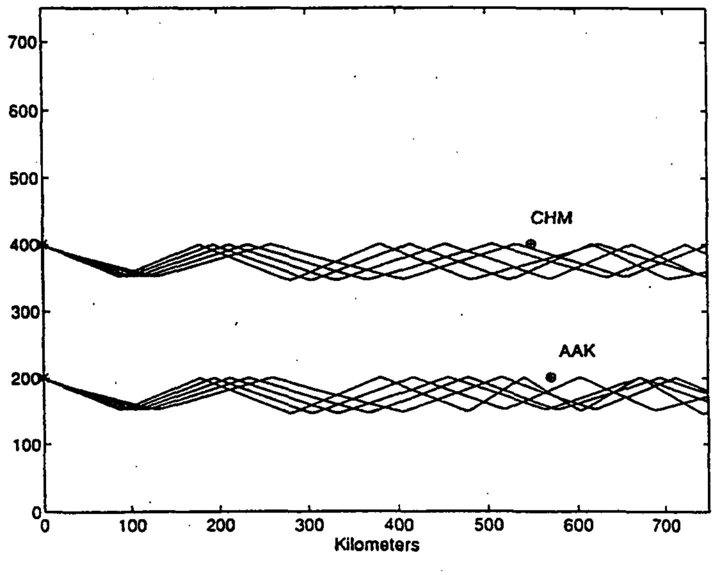

Figure 2. Top left: record section of event #3, 6 May 92. Data were band passed filtered 1-5 Hz.

Figure 3. Top right: map view of bounce points from dynamic ray tracing for event #3. Wave front remains coherent for 5 turning rays in the Moho transition.

Figure 4. Bottom: rays for event #3 for a range of vertical take-off angles of 61-69 degrees for paths to stations AAK and CHM. Due to the relatively flat Moho along the ray path, the turning rays in the Moho transition remain similar in form to a horizontal range of 500-600 km.

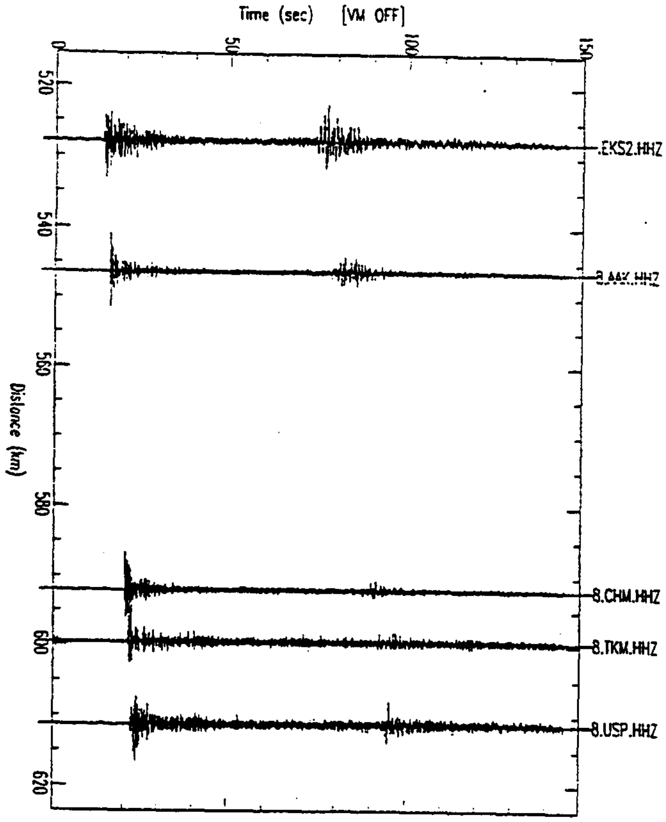

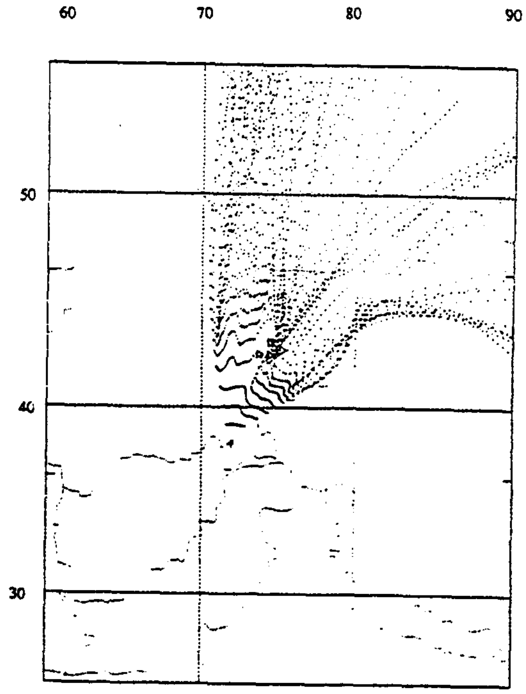

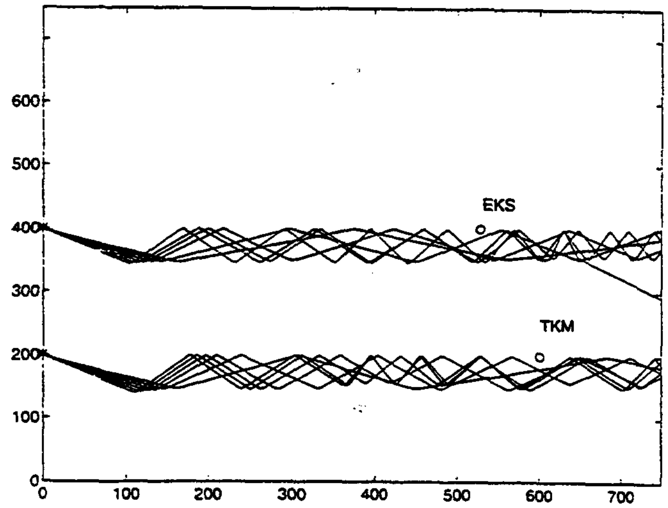

Figure 5 Top left: record section of event #1, 6 May 92. Data were band passed filtered 1-5 Hz. The signals vary greatly across the array; station TKM has little or no Lg.

Figure 6. Top right: map view of ray bounce points from dynamic ray tracing for event #1. The wavefront is strongly affected by the steep Moho topography. A casutic surface appears to pass through the middle of the array.

Figure 7. Bottom: rays for event#1 at vertical take-off angles of 63-71 degrees for paths to stations TKM and EKS2. Both paths show focusing and defocusing due to gradients in Moho topography.

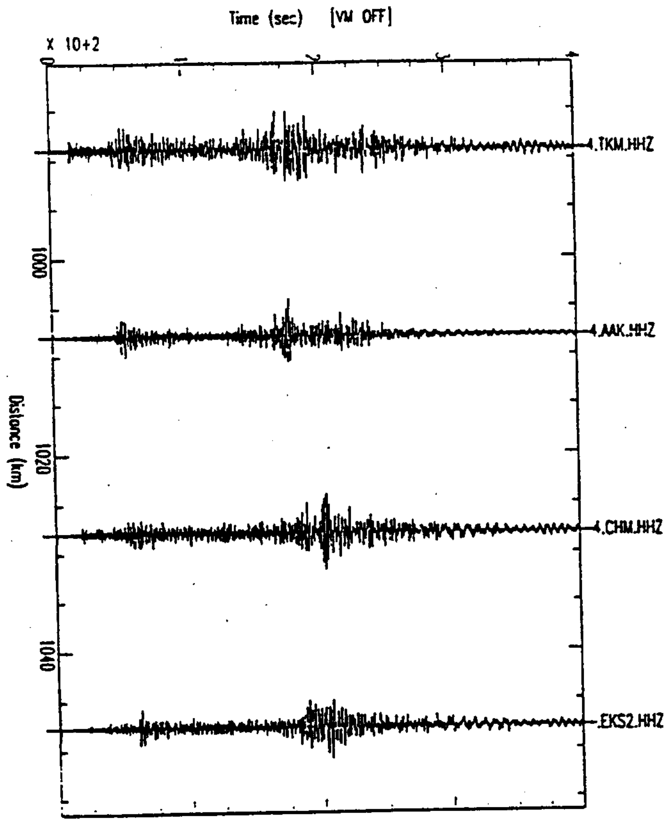

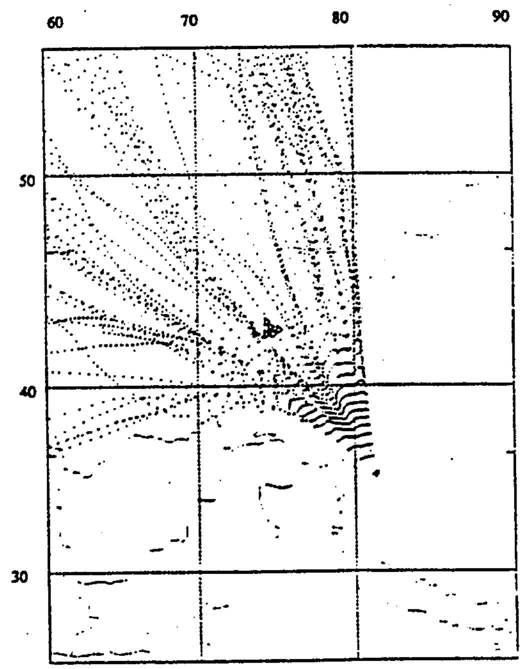

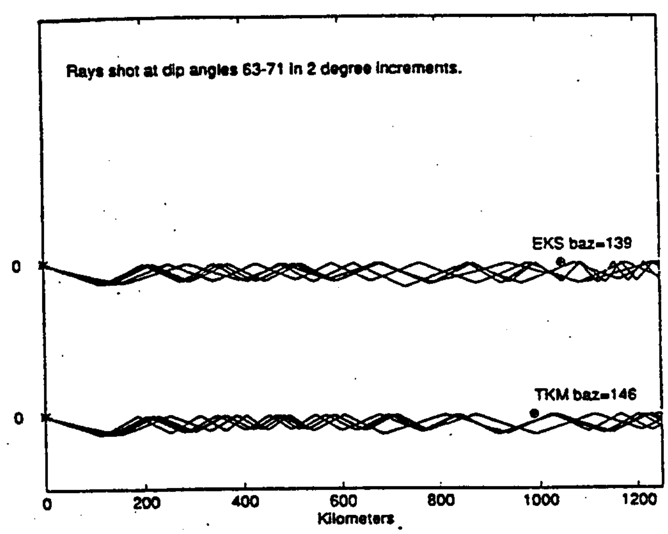

Figure 8 Top left: record section of event #2, 6 May 92. Data were band passed filtered 1-5 Hz. The Lg coda varies across the array.

Figure 9 . Top right: map view of ray bounce points from dynamic ray tracing for event #2. Rays beend sharply due to steep gradients in the Moho.

Figure 10 Bottom: rays for event #2 at vertical take-off angles of 63-71 degrees for paths to stations TKM and EKS2. Both paths show development of focusing and defocusing due to gradients in the Moho topography.